Plant, Cell & Environment

WILEY

Plant, Cell & Environment

ORIGINAL ARTICLE

Fatty Acid Desaturases GmROD1s Are Involved in Nodulation by Regulating the Flux of Polyunsaturated Fatty Acids

Wenying Liao[1,2] | Jie Li[1,2] | Runze Guo[1,2] | Juan Xu[1] | James Whelan[1,2] | Huixia Shou[1,2]

[1]State Key Lab of Plant Environmental Resilience, College of Life Sciences, Zhejiang University, Hangzhou, Zhejiang, China | [2]The Provincial International Science and Technology Cooperation Base on Engineering Biology, International Campus of Zhejiang University, Haining, Zhejiang, China

Correspondence: Huixia Shou (huixia@zju.edu.cn)

Received: 20 December 2025 | **Revised:** 12 March 2026 | **Accepted:** 22 April 2026

ABSTRACT

Legume–rhizobia symbiosis requires induction of fatty acid (FA) biosynthesis, especially the polyunsaturated fatty acids (PUFAs), as essential lipid and membrane components for nodulation. However, the regulation of PUFA homoeostasis remains poorly understood. Direct molecular and genetic evidence linking specific FA desaturation enzymes to this process is limited. Here, we investigated two soybean FA desaturation genes, *GmROD1a/b*, and provided their previously unrecognised roles in nodulation. Both were strongly induced during early rhizobial infection and remained highly expressed throughout nodule development. Overexpression significantly enhanced nodulation and plant growth, whereas disruption reduced nodule numbers. Transcriptomic analyses further revealed that GmROD1s promote PUFA accumulation and regulate genes associated with nodulation and nodule function, energy metabolism, membrane biogenesis, etc. We also identified two members of the WRINKLED family of transcription factors that are co-expressed with *GmROD1* in rhizobia-infected roots and nodules. Further, promoter binding and transcription activation assays confirmed that GmWRI1 and the newly identified nodulation-associated factor, GmWRI3, directly promote *GmROD1a/b* expression, and overexpression of either transcription factor in soybean hairy roots significantly promoted nodulation. Together, our study uncovers a previously unappreciated role of ROD1 in nodulation, extending the functional role beyond FA desaturation. More importantly, we provide new molecular evidence linking nodulation to PUFA biosynthesis mediated by a previously unappreciated *GmWRI1/3–GmROD1a/b* regulatory module. Notably, the biological function of *GmWRI3* in soybean has not been experimentally characterised. These findings establish a mechanistic connection between fatty acid metabolism and nodulation, offering potential targets for improving legume crop yields.

1 | Introduction

Symbiotic nitrogen fixation (SNF) in legumes is characterised by plants providing a hospitable environment and carbohydrates to the microorganisms, which, in return, convert atmospheric nitrogen into a form usable for plant growth. SNF plays a pivotal role in enhancing soil fertility, reducing the need for synthetic fertilisers, and increasing yield, especially in crops like soybean [*Glycine max* (L.) Merr]. Elucidating the molecular mechanisms underlying these processes remains a central objective in legume biology.

Legume–rhizobia symbiosis is an efficient way to promote plant growth and improve crop production (Andrews and Andrews 2017). For example, overexpression of the phosphate transporter *GmPT7* enhances nodulation and shoot nitrogen content, resulting in a yield increase of up to 36% (Chen et al. 2019). In addition, field inoculation with rhizobia markedly improved soybean yield compared with the non-inoculated control (Qin et al. 2012). Likewise, overexpression of *GmHSP17.9*, which is specifically induced in infected nodule tissues, increases nodule numbers and total nitrogen content (Yang et al. 2022). These studies highlight the importance of

host metabolic and regulatory pathways in supporting symbiotic development. However, how lipid metabolic processes are integrated into the genetic control of nodulation remains incompletely understood.

Fatty acid (FA) biosynthesis has emerged as a key metabolic determinant of symbiotic interactions. Host-derived FAs serve as major carbon sources for symbiotic microbes (Jiang et al. 2017) and are required for intracellular accommodation of endosymbionts (Rich et al. 2021). In arbuscular mycorrhizal symbiosis, key FA biosynthetic genes—including *WRI*, *KAS II*, and *ACP*—are transcriptionally activated during fungal colonisation, and their manipulation alters mycorrhizal symbiosis efficiency (Bravo et al. 2016, 2017; Jiang et al. 2017; Brands et al. 2018; Rich et al. 2021). In soybean, lipidomic and transcriptomic analyses of infected roots and developing nodules further indicate that membrane lipid biosynthesis and FA transport are strongly induced during soybean–rhizobia symbiosis (Upchurch 2008; Brechenmacher et al. 2010; Bourassa et al. 2017; Zhang et al. 2020). Consistent with these observations, genetic manipulation of FA biosynthetic components affects nodulation outcomes. For example, Silencing of FA biosynthetic genes such as *GmACP* reduces FA levels and suppresses nodule formation (Wang et al. 2014), whereas loss of *SACPD* disrupts FA composition and nodule morphology (Gillman et al. 2014; Lakhssassi et al. 2020). Overexpression of *GmWRI1* in soybean hairy roots enhances root glycolysis and lipid biosynthesis and promotes nodule formation (Chen et al. 2020; Zhang et al. 2020). Collectively, these findings support a model in which lipid metabolism contributes to the cellular remodelling required for symbiotic development.

A large demand for polyunsaturated fatty acids (PUFAs) and membrane biogenesis occurs during soybean–rhizobia symbiosis, which plays an irreplaceable roles in defence and membrane fluidity during rhizobial inoculation (Upchurch 2008; Brechenmacher et al. 2010). However, a critical knowledge gap remains: despite extensive transcriptomic and lipidomic evidence linking PUFA dynamics to nodulation, the specific enzymatic steps that channel polyunsaturated fatty acid (PUFA) flux during nodulation remain poorly defined. In particular, the phosphatidylcholine:diacylglycerol cholinephosphotransferase (PDCT) enzymes encoded by *ROD1*, key regulators of PUFA desaturation and flux into TAGs, have not been investigated in the context of nodulation. The PDCT catalysers the transfer of oleic acid (18:1) from diacylglycerol (DAG) to phosphatidylcholine (PC) for desaturation into linoleic acid (C18:2) and linolenic acid (C18:3), and also the reverse reaction of the acyl groups back to DAG. Loss of ROD1 function in *Arabidopsis* reduces C18:2 and C18:3 accumulation in the seeds by 40% (Lu et al. 2009). Overexpression of the *PDCT* gene increased carbon flux toward triacylglycerol (TAG) synthesis, exhibiting significant increases in seed yield, seed oil content and oil yield per plant (Abdullah et al. 2024). The important role of ROD1 and its encoded enzyme PDCT in crops has also received some attention. In rapeseed, ROD1 catalysers a major flux of PUFAs in seed oil synthesis, with seeds of the double *BnROD1.A3/C3* mutant containing approximately significantly reduced PUFAs (Bai et al. 2020). In rice, a genome-wide association study (GWAS) of rice found that gene encoding a PDCT enzyme, *OsLIN6*, significantly affected the natural variation of FA composition and showed variability among subpopulations. Population genetic analysis showed that a specific *OsLIN6* has been selected in *japonica* rice, resulting in significantly higher PUFAs in rice seeds than in *indica* rice (Zhou et al. 2021). In soybean, a study through GWAS analysis found that genetic variation of *GmROD1* alters seed total FA content (Fang et al. 2017). Loss function of *GmROD1* resulted in significant decreases in seed PUFA content (Li et al. 2023), and heterologous expression of *GmPDCT*s restores lipid phenotypes in Arabidopsis mutants (Ulch et al. 2025). Despite these advances, whether *ROD1* participates in legume nodulation has not been investigated.

In this study, we identified two *GmROD1* genes that showed high expression levels in the soybean nodules and seeds. Given the need for membrane biogenesis during symbiotic development, as well as the potential roles for PUFAs, we were intrigued by the ideas that ROD1 may play previously unrecognised roles in soybean nodulation, which is really different from ROD1's function in other species. Here, we functionally characterise *GmROD1a/b* and demonstrate that their roles in regulating PUFA flux into TAGs, enhance nodulation, increase nitrogenase activity, and ultimately improve plant growth. These findings expand the functional context of ROD1 beyond seed lipid metabolism and provide new insight into how fatty acid remodelling is integrated into the molecular regulation of nodulation.

2 | Materials and Methods

2.1 | Plant Materials and Growth Conditions

Soybean cultivar Williams 82 was used for gene cloning, gene expression and functional analysis of *GmROD1*s and *GmWRI*s. One *gmrod1a/b* double mutant line was obtained using CRISPR/Cas9-mediated genome editing technology (The target sequence (5′-GCTGAGGGTGGGGAGCTTGA-30) was designed in a region conserved in both *GmROD1a* and *GmROD1b*), and three *GmROD1a* overexpression lines driven by its native promoter were generated in the Williams 82 background through *Agrobacterium tumefaciens* (*LBA4404*)-mediated cotyledon node transformation system.

In this study, various cultivation conditions were employed to meet different experimental requirements. For cultivation in soil, soybean plants were grown in 3-L pots filled with sterilised nutrient soil in the greenhouse (28°C/24°C day/night temperature, 15 h/9 h light/dark, 800 $\mu mol\ m^{-2}\ s^{-1}$ light intensity and relative humidity of 60%–80%), watering with nitrogen-deficient (0.05 mM) nutrition solutions and inoculating with rhizobia. Field trials for soybean were conducted at two locations: the experimental field of the Zhejiang University International Campus, Haining (30.53° N, 120.69° E), and the Zhejiang University (Hainan) Advanced Technology and Industrial Innovation Platform (18.43° N, 109.17° E). Plants were grown under standard agronomic conditions. According to the experiment design, nitrogen fertilisation was applied in doses of 30 $kg\ ha^{-1}$ (ammonium nitrate 34%). All fertilisation was done before sowing. For cultivation in nutrient solution, soybean seeds were germinated on wet filter paper for 5 days. The seedlings were transferred to box, the full-nutrient hydroponic solution for soybean was prepared based on half-strength Hoagland's solution with slight modifications: 1.5 mM K_2SO_4, 2.5 mM $CaCl_2{\cdot}2H_2O$,

1.0 mM $MgSO_4 \cdot 7H_2O$, 0.38 μM $ZnSO_4 \cdot 7H_2O$, 1.57 μM $CuSO_4 \cdot 5H_2O$, 0.09 μM $(NH_4)_6Mo_7O_{24} \cdot 4H_2O$, 23.13 μM H_3BO_3, 4.57 μM $MnCl_2 \cdot 4H_2O$, 0.25 mM KH_2PO_4, and 0.1 mM Fe(II)-EDTA with 2.5 mM (+N) or 0.05 mM (−N) KNO_3, adjusted to pH 5.8. For cultivation in vermiculite, the soybean seeds were germinated and cultivated in sterile vermiculite in the greenhouse, and watered with different nutrient solutions according to the needs of the experiment.

2.2 | Soybean Hairy Root Transformation

Chimeric soybean plants are composites of wild-type shoots and transgenic hairy roots. The hypocotyl injection method (Kereszt et al. 2007; Guo et al. 2011) was used for hairy root transformation, with some modifications. Briefly, hypocotyls of 6-day-old seedlings with unfolded cotyledons were infected with *Agrobacterium rhizogenes* strain K599 carrying the transgene construct and removed the main roots. Inoculated plants were kept under high-humidity vermiculite until the emerged hairy roots reached the length of 5 cm. The herbicide (20% glufosinate) was diluted 1:500 and applied for the selection of positive transgenic hairy roots, which were then used for further nodulation assays.

2.3 | Grafting

Stable transgenic lines of *GmRod1a*-OE, mutant *gmrod1a/b* and wild type were used in grafting experiments with different shoot and root combinations. Grafting was carried out 5–7 days after sowing using a wedge-shaped graft with the cotyledons left on the scion (Delves et al. 1986), with minor modifications. Grafts were held in place by tape and sticks and covered with plastic bags in the dark. Five days after grafting, the bags were removed, and then the grafted plants were inoculated with *USDA110*. We grew the grafted plants in vermiculite, inoculated them with rhizobia, and irrigated with a nitrogen-deficient nutrient solution. Grafted plants were kept moist to prevent desiccation until the grafts had functionally rejoined.

2.4 | Nodulation Assay

Soybean seeds were sterilised with chlorine gas for 12–14 h. Five-day-old seedlings were inoculated with the rhizobium USDA110 for nodulation assays. Seedlings were inoculated with rhizobia for 1 h (OD_{600} was adjusted at 0.8–1.0) and transplanted to a nutrient solution at pH 5.8 with ±N concentrations. Nodule phenotypes were evaluated 21 days post-inoculation (dpi).

For nodulation assays of transgenic composite plants and grafted plants, plants were transplanted to pots containing vermiculite. The plants were inoculated with 30 mL USDA110 suspended in distilled water ($OD_{600} = 0.1$). Plants were watered with the −N solution.

2.5 | Histochemical Analysis

A 2-kb fragment upstream of ATG was cloned into the pBI vector to generate the *proROD1a*-GUS transgenic plants. For histochemical GUS analysis, various soybean tissues were incubated in GUS staining solution (50 mM sodium phosphate pH 7.0, 10 mM EDTA, 20% (v/v) methanol, 0.1% (v/v) Triton X-100, 1 mM potassium ferrocyanide, 1 mM potassium ferricyanide, and 2 mM 5-bromo-4-chloro-3-indole-beta-glucuroniude (X-Gluc) dissolved in dimethyl sulfoxide) at 37°C in the dark. Chlorophyll was removed by incubation in 70% (v/v) ethanol at room temperature.

Toluidine blue staining: Nodule sections were stained in 1% toluidine blue buffer (anhydrous ethanol dissolved, 1% (w/v) NaCl solution diluted) for 2 min, decolorised with 0.5% (v/v) glacial acetic acid solution for 1 min, and finally rinsed with ultrapure water.

Observations were performed using a light microscope (Mantis-Elite).

2.6 | Subcellular Localisation in Soybean Protoplasts

To analyse the subcellular localisation of GmROD1 proteins, the *pSAT6-35S:GmROD1a-YFP* and *pSAT6-35S:GmROD1b-YFP* constructs were introduced into protoplasts derived from soybean leaves. For preparing the protoplasts, soybean seedlings were grown in a greenhouse for 10 days. After harvesting the soybean protoplasts, soybean protoplast transformation was performed as described previously (Wu and Hanzawa 2018). YFP and mCherry fluorescence signals in soybean mesophyll protoplasts were detected using an LSM710 NLO confocal laser scanning microscope (Zeiss, Jena, Germany).

2.7 | Quantitative Real-Time RT-PCR Analysis

For quantitative real-time PCR analysis, the soybean housekeeping gene *GmACTIN* (*Glyma.15g034000*) and *GmCYP2* (*Glyma.12G024700*) were used as a reference genes. The primer sequences are given in Supporting Information S2: Table 1. Total RNA was extracted from soybean tissues using RNeasy Plant Mini Kit (Tiangen). The RNA was treated with RNase-free DNase I to remove contaminating genomic DNA before synthesising first-strand cDNA using MMLV reverse transcriptase (Promega), according to the manufacturer's instructions. The cDNA products were used as templates. All reactions were performed on a Bio-Rad CFX system (Bio-Rad, USA) for 40 cycles (94°C for 30 s, 56°C for 30 s and 72°C for 30 s). Gene-specific primers are listed in Supporting Information S2: Table 1. All amplification reactions were performed with three biological replicates and two technical replicates.

2.8 | FA Content and Lipid Analysis

Seeds (50 mg), root (100 mg) and nodule (50 mg) tissue samples were prepared for FA isolation. The FA extraction method was performed as described by Liao et al. (2024) without modification. All experiments conducted with three biological replicates. Lipid profile analysis was performed using HPLC–MS following the method described by Liao et al. (2024), with six biological replicates.

2.9 | Ureide Content Assays

To determine ureide concentrations in soybean, 50 mg of lyophilised leaf tissue was used. The tissue was homogenised in 1 mL of ice-cold H_2O and centrifuged at 15 000 × *g* for 30 min at 4°C. The supernatant (100 μL) was used for total ureide assays by mixing with 100 μL 0.5 M NaOH, followed by heating at 100°C for 8 min. After cooling on ice for 5 min, samples were mixed with 10 μL of 0.65 M HCl and 10 μL of phenylhydrazine. After 5 min at room temperature, samples were placed on ice, and mixed with 50 μL of ice-cold concentrated HCl and 10 μL of potassium ferricyanide solution (50 mg in 3 mL of water). Samples were placed at room temperature for at least 15 min, followed by centrifugation at 15 000 × *g* for 10 min. The absorbance of supernatant was measured using a spectrophotometer at 535 nm.

2.10 | Yeast One-Hybrid Assay

Yeast one-hybrid assays were performed using a Matchmaker Gold Yeast One-Hybrid System (Clontech). The full length *GmWRI1* and *GmWRI3* coding sequences were amplified from soybean cDNA and then cloned into the pGADT7 expression vector. The promoters of the *GmROD1* genes were cloned into the pHIS2 vector. The prey and bait plasmids were co-transformed into the Y187 strain according to the manufacturer's instructions. The pGADT7-p53 and pHIS2-p53 were used as the positive control, empty vector pGADT7-rec2 with pHIS2 was used as a control for excluding the self-activation, pGADT7-candidate proteins with empty pHIS2 vector and pHIS2-candidate promoters with empty pGADT7 vector were used as negative controls. 3-Amino-1,2,4-triazole (3-AT; 120 mM) was used to screen the minimal inhibitory concentration for the bait strains.

2.11 | Chromatin Immunoprecipitation (ChIP) Assay

Transgenic hairy roots (12 dpi) expressing *35S*:*GmWRI1-FLAG* or *35S*:*GmWRI3-FLAG* were used for ChIP assays. Tissues were crosslinked with 1% formaldehyde at room temperature for 30 min and neutralised with 0.125 M glycine. Roots were ground to a fine powder in liquid nitrogen and nuclei were isolated. EpiQuik Plant ChIP (EPIGENTEK) kit was used for immunoprecipitation according to the manufacturer's protocol. Immunoprecipitation was carried out using anti-FLAG (Invitrogen) antibodies. Chromatin precipitated without the use of antibodies was used as a negative control, while chromatin collected prior to immunoprecipitation was used as an input control. qPCR analysis was performed, and enrichment was normalised to the corresponding input DNA, and the enriched foldchanges were normalised to CK (afragment without any predicted binding motif).

2.12 | Transcriptional Activation Assay in *N. benthamiana* Leaves

The promoters (a 2-kb fragment upstream of ATG) of *GmROD1a* and *GmROD1a* were cloned into *pCAMBIA1300-LUC* as reporters. The full-length ORF of *GmWRI*s were cloned and inserted into a *pCAMBIA1300* vector under the control of the 35S promoter as effectors. The LUC gene driven by the 35S promoter was used as negative control. *Agrobacterium* strain GV3101 was used in the experiments. Effectors and reporters were co-transfected into tobacco leaves. Then, placed the leaves in the chemiluminescence/fluorescence image analysis system (Tanon-5200, China) to observe and capture LUC fluorescence images 3 days after infiltration, and the Indigo software was used to quantify the chemiluminescence intensity. The LUC activities were normalised to those infiltrated with an empty vector.

2.13 | Transcriptomics

Roots (5 api) and nodules (30 dpi) of WT, *gmrod1a*/b and *GmROD1a-OE* lines were collected for RNA-seq library preparation and transcriptome sequencing. The whole procedure was followed by (Liao et al. 2024) with light modification. RNA purification, reverse transcription, library construction and sequencing were performed at Shanghai Majorbio Bio-pharm Biotechnology Co. Ltd. (Shanghai, China) according to the manufacturer's instructions (Illumina, San Diego, CA). Each line was analysed in three biological replicates. To identify DEGs (differential expression genes) between two different samples, the expression level of each transcript was calculated according to the transcripts per million reads (TPM) method. RSEM was used to quantify gene abundances. Essentially, differential expression analysis was performed using DESeq. 2 or DEGseq. DEGs with $|\log2FC| \geqq 1$ and FDR ≤ 0.05(DESeq. 2) or FDR ≤ 0.001(DEGseq) were considered to be significantly different expressed genes. In addition, functional-enrichment analysis, including GO and KEGG, was performed to identify which DEGs were significantly enriched in GO terms and metabolic pathways at a Bonferroni-corrected p-value ≤ 0.05 compared with the whole-transcriptome background. GO functional enrichment and KEGG pathway analysis were performed using Goatools and KOBAS, respectively.

3 | Results

3.1 | *GmROD1* Genes Are Highly Expressed in Rhizobia-Inoculated Roots, Nodules and Developing Seeds

To assess the functions of the two homologous genes of *AtROD1* in soybean (Supporting Information S1: Figure 1), *GmROD1a* (*Glyma.07G029800*) and *GmROD1b* (*Glyma.08G213100*), we examined the expression patterns of *GmROD1* across various soybean tissues. Notably, both genes exhibited high expression levels in developing seeds and nodules (Figure 1 and Supporting Information S1: Figure 2). To gain deeper insights, transgenic soybean plants carrying a GUS reporter driven by the *GmROD1a* promoter were subjected to histochemical staining. Strong GUS activity was detected in nodules and during seed development (Figure 1D and Supporting Information S1: Figure 2C).

To confirm our hypothesis that GmROD1s may be involved in soybean–rhizobia symbiosis or nodule development based on the expression pattern, we specifically analysed the expression of *GmROD1a/b* in roots under −/+ *rhizobium* (USDA110)

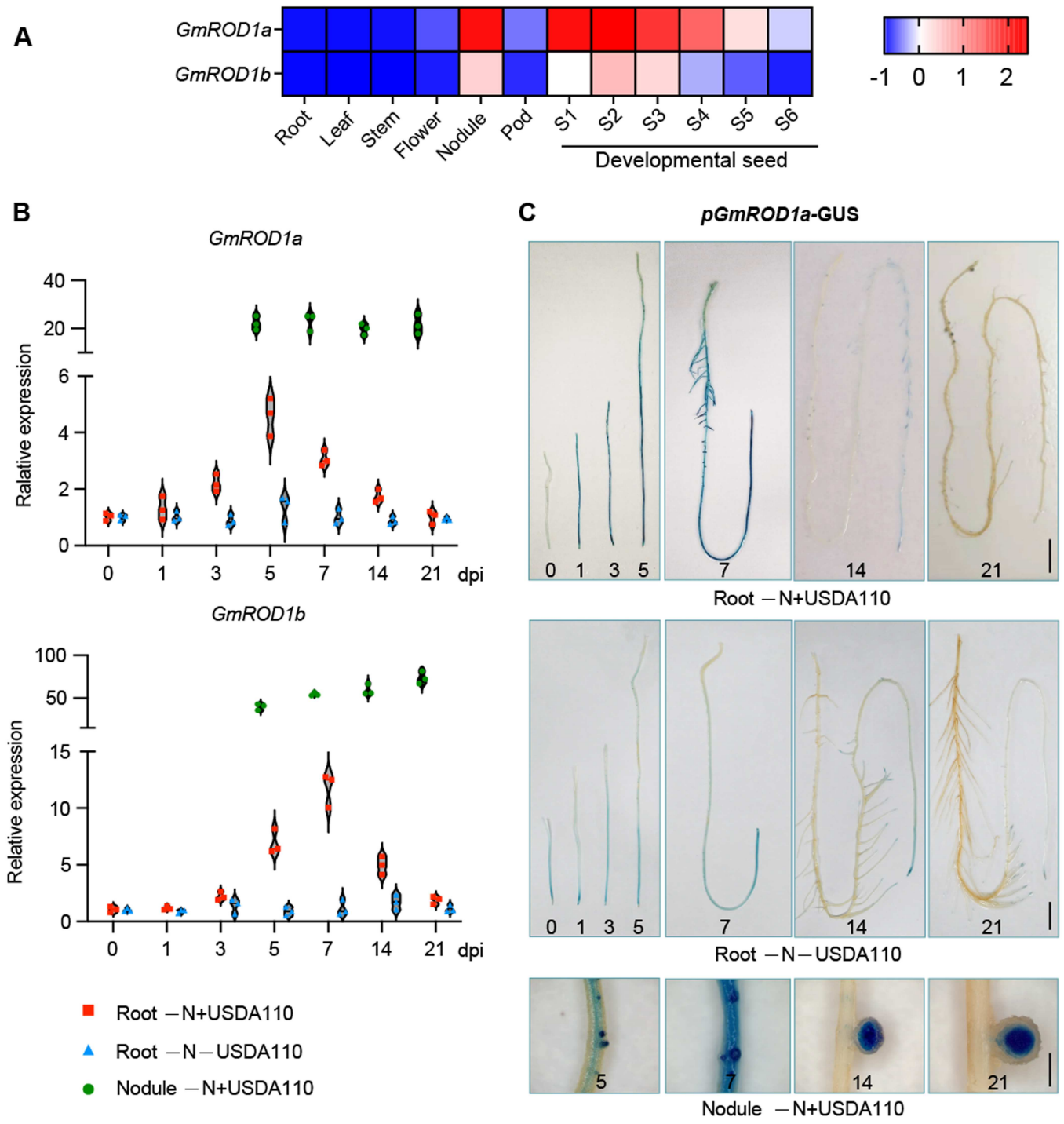

FIGURE 1 | Expression patterns of GmROD1a and GmROD1b in soybean plants. (A) qRT-PCR analysis of *GmROD1a* and *GmROD1b* transcript levels in different soybean tissues and different development stages of seeds. Stage 1 (1): 40–60 mg; Stage 2 (S2): 80–110 mg; Stage 3 (S3): 180–220 mg; Stage 4 (S4): 280–330 mg; Stage 5 (S5): 350–400 mg; Stage 6 (S6): 420–470 mg. Data were expressed as means ± SD. Data are based on qRT-PCR expression analysis, with transcript abundance normalised relative to *GmACTIN* in the respective tissues (Experiments were conducted with three biological and two technical replicates.) For visualisation, mean expression values across replicates were calculated and subsequently normalised to generate z-scores for each gene across tissues. (B) The expression levels of *GmROD1a* and *GmROD1b* in soybean roots and nodules over 21 days after inoculation with *Bradyrhizobium japonicum* (USDA110) under nitrogen sufficient or deficient conditions. Experiments were conducted with three biological and two technical replicates. The relative expression was normalised to the expression level of *GmROD1*(Root −N + USDA110, 0 dpi). (C) GUS activity driven by the *GmROD1a* promoter in soybean roots and nodules with or without rhizobial inoculation. Scale bar in root images, 1 cm; scale bar in nodule images, 5 mm. DAI: days after inoculation; −N + USDA110: under deficient N condition with rhizobial infection; −N–USDA110: under deficient N condition without rhizobial infection. [Color figure can be viewed at wileyonlinelibrary.com]

inoculation conditions. qRT-PCR and histochemical analyses showed that, under deficient N condition (−N), the abundance of *GmROD1* transcripts in roots were sharply increased and peaked as new nodules emerged within 7 days post-inoculation (dpi), but the induction was absent in non-infected roots (−USDA110) (Figure 1B–D). Furthermore, strong GUS activity was detected in the nitrogen fixation zone throughout the whole nodule formation process (Figure 1D and Supporting Information S1: Figure 2C). These results indicate that *GmROD1s* play a role in nodule initiation or development.

3.2 | GmROD1s Contribute to Nodulation

To elucidate the function of GmROD1s, we generated three *GmROD1a* overexpression lines and one double mutant, *GmROD1-OE1/2/3* and *gmrod1a/b*, respectively (Supporting Information S1: Figure 3). To further explore the role of GmROD1s in soybean–rhizobia symbiosis, different plants grown in a greenhouse were inoculated with rhizobia and cultured in a nutrient solution containing sufficient nitrogen (+N) or deficient nitrogen (−N) for nodule phenotypic analysis (Figure 2A). Overexpression of *GmROD1a* in soybeans resulted in more nodules and promoted nodule growth, compared to the WT plants. Conversely, the *gmrod1a/b* mutant exhibited a reduction in nodule count and dry weight (Figure 2C,D).

Ureides, like allantoin and allantoic acid, are the principal output products of nitrogen fixation, and are used as markers of nitrogen-fixing ability (Tegeder 2014). Ureide content measurements validated these findings, with higher levels detected in *GmROD1a*-OE lines and reduced levels in *gmrod1a/b* mutants under −N conditions (Figure 2E). *GmROD1a*-overexpression plants exhibited markedly higher nitrogen content compared to WT plants in the presence of rhizobia. Conversely, mutants displayed a decrease in nitrogen content, accompanied by significantly impaired growth (Figure 2A,C). Furthermore, we employed a strategy involving chimeric

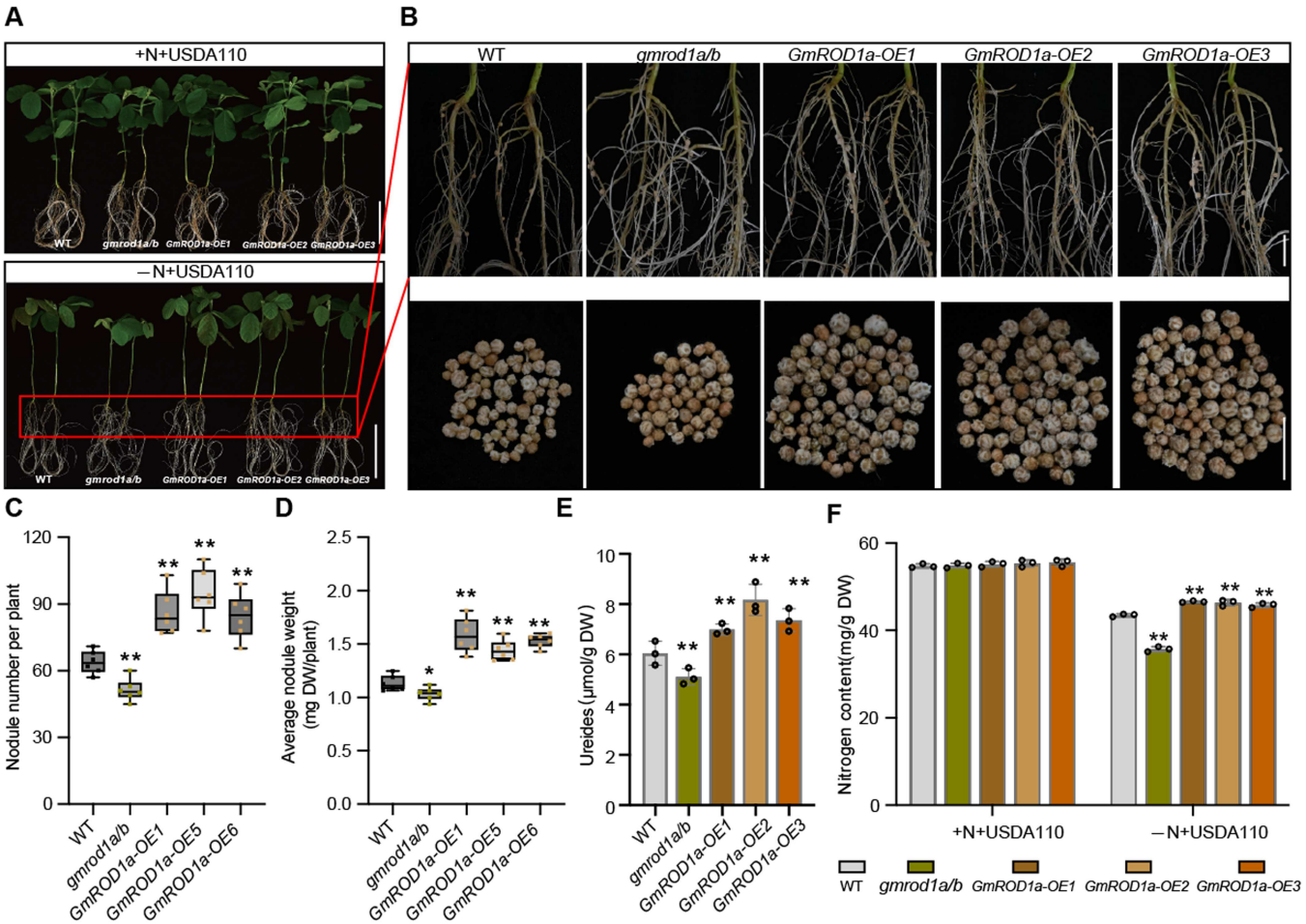

FIGURE 2 | Growth performance and nodule phenotypes of WT, gmrod1a/b mutants and GmROD1a-overexpression plants after rhizobial inoculation. (A) Growth performance of WT, *gmrod1a/b* mutant and *GmROD1a*-overexpression plants inoculated with *Bradyrhizobium japonicum* USDA100 rhizobia were grown at sufficient N condition or deficient N condition. Scale bar, 10 cm; sufficient N and sufficient N were 50 μM and 2.5 mM N, respectively. (B–D) Nodule phenotype (B) on roots (above) and after excision (below), nodule number (C), and dry weight (D) of WT, *gmrod1a/b* mutant and *GmROD1a*-overexpression plants inoculated with rhizobia under deficient N condition. Scale bar, 1 cm. Seedlings were inoculated with USDA110 5 days after germination. Plants were grown in nutrient solution with one of two N levels for 21 days. $n = 6$. (E, F) Ureide content (E) and nitrogen content (F) in nodules of WT, *gmrod1a/b* mutant and *GmROD1a*-overexpression plants. Soybean leaves were harvested 21 days after infection; $n = 3$. Data are the means ± SD; significant differences ($^*p < 0.05$, $^{**}p < 0.01$) based on Student's *t*-test compared with WT are indicated by asterisks. [Color figure can be viewed at wileyonlinelibrary.com]

soybean plants with *GmROD1a*- and *GmROD1b*-overexpressing hairy roots, which demonstrated that *GmROD1b* in soybean acts as the same function as *GmROD1a* (Supporting Information S1: Figure 10). Collectively, the changes in nodule formation observed in *GmROD1*-overexpression corroborate the crucial role of GmROD1s in the soybean–rhizobia symbiosis.

3.3 | GmROD1s Direct Flux of Polyunsaturated Fatty Acids Into Triacylglycerols

Main PC-to-DAG conversion is catalysed by ROD1 through the phosphocholine headgroup exchange between PC and DAG for FA desaturation during TAG biosynthesis in the endoplasmic reticulum (ER) (Bates et al. 2012). ROD1 is responsible for the major fluxes of 18:1 into the PC pool and the release of PUFA from PC for TAG synthesis (Figure 3A). To validate this localisation, soybean protoplasts were transfected with a construct expressing *35S:GmROD1-YFP* fusion, along with an ER marker. As anticipated, the resulting fluorescence signals demonstrated co-localisation with the ER marker (Supporting Information S1: Figure 2D), confirming GmROD1s as ER proteins, consistent with the location of FA desaturation.

To further confirm the biochemical function of GmROD1s, we analysed FA profiles in different tissues. Results showed that altering the expression level of *GmROD1* genes in soybean changed the FA profiles. Overexpression of *GmROD1a* led to an increase in linoleic acid (18:2), a PUFA, by 5.2% in inoculated roots (5 dpi), 18.6% nodules, and 3.5% in seeds, while the oleic acid (18:1) substantially decreased, when compared to the WT (Figure 3B–D), showing opposite trends in mutant. Moreover, we performed lipid analysis of the roots (5 dpi) and nodules (30 dpi) from both WT and *GmROD1a*-overexpression lines (*GmROD1a-OE*). In contrast with the increases in 18:2/3-DAG and 18:2/3-TAG in *GmROD1a-OE*, the 18:1-DAG and 18:1-TAG levels were significantly decreased in both roots and nodules of the *GmROD1a-OE* plants (Figure 3E,F). Overall, these findings

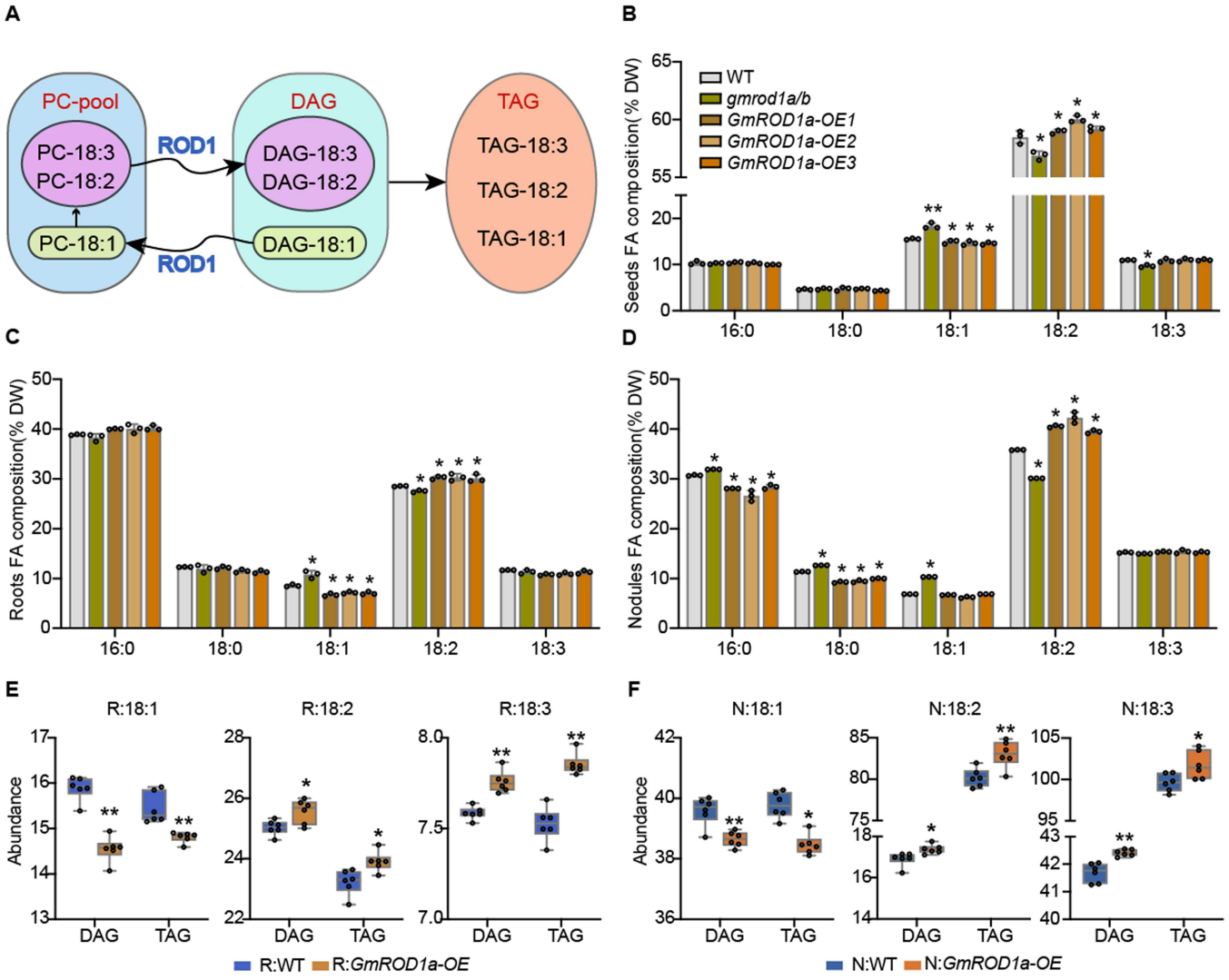

FIGURE 3 | GmROD1s regulate PUFAs accumulation in the endoplasmic reticulum. (A) Catalytic diagram of *GmROD1a/b*-encoded phosphatidylcholine:diacylglycerol cholinephosphotransferase (PDCT) enzyme converting acyl groups between phosphatidylcholine (PC) and diacylglycerol (DAG). (B–D) FA composition in seeds (B), in roots (5 DAI) (C), and in nodules (30 DAI) (D) in WT (blue), *gmrod1a/b* mutant (green) and *GmROD1a* overexpression lines (oranges). DW: dry weight; $n = 3$. (E, F) The abundance of DAGs and TAGs extracted from roots 5 DAI (E) and in nodules 30 DAI (F) in WT and a *GmROD1a* overexpression line. ($n = 6$). Data are shown as the means ± SD; significant differences (*$p < 0.05$, **$p < 0.01$) based on Student's *t*-test compared with WT are indicated by asterisks. [Color figure can be viewed at wileyonlinelibrary.com]

demonstrate the involvement of the GmROD1s in regulating the flux of PUFAs into TAGs.

3.4 | Changes in GmROD1 Expression Modulate Gene Networks Associated With Lipid Metabolism and Nodulation

To further elucidate the functional contribution of GmROD1 in rhizobial inoculation, roots at 5dpi and nodules at 30 dpi were collected from WT, *gmrod1a/b* mutant and *GmROD1a-OE* plants for RNA extraction and sequencing. Clean reads from RNA-sequencing were mapped onto the soybean genome, and genes showing at least a twofold increase or a 50% decrease relative to WT were defined as differentially expressed genes (DEGs). DEGs in roots (R) and nodules (N) from each comparison of WT versus *gmrod1a/b* or *GmROD1a-OE* were designated as R/N: *gmrod1a/b* versus WT and R/N:*GmROD1a* versus WT, respectively (Figure 4A).

In roots, both GmROD1a-OE and *gmrod1a/b* exhibited enrichment in Gene Ontology (GO) categories related to the nitrate/nitrogen response pathway and lipid metabolism, including 'response to nitrate', 'response to nitrogen compound', and 'nitrate transport' (Supporting Information S1: Figure 7A,B). Notably, DEGs annotated under the enriched GO terms 'response to nitrate' and 'nitrate transmembrane transport' were all upregulated in *GmROD1a-OE* but downregulated in the *gmrod1a/b* mutant (Figure 4B). In addition, DEGs associated with the significantly enriched GO term 'lipid metabolic process' were all downregulated in the mutant but highly expressed in *GmROD1a-OE* (Figure 4C). In nodules, significantly enriched GO terms in N:*gmrod1a/b* versus WT included nitrogen, carbohydrate and lipid metabolic processes, as well as membrane-related processes, especially DEGs in N:*GmROD1a* versus WT were predominantly enriched in membrane-related categories (Supporting Information S1: Figure 7D). Notably, both comparisons showed significant enrichment for lipid metabolic

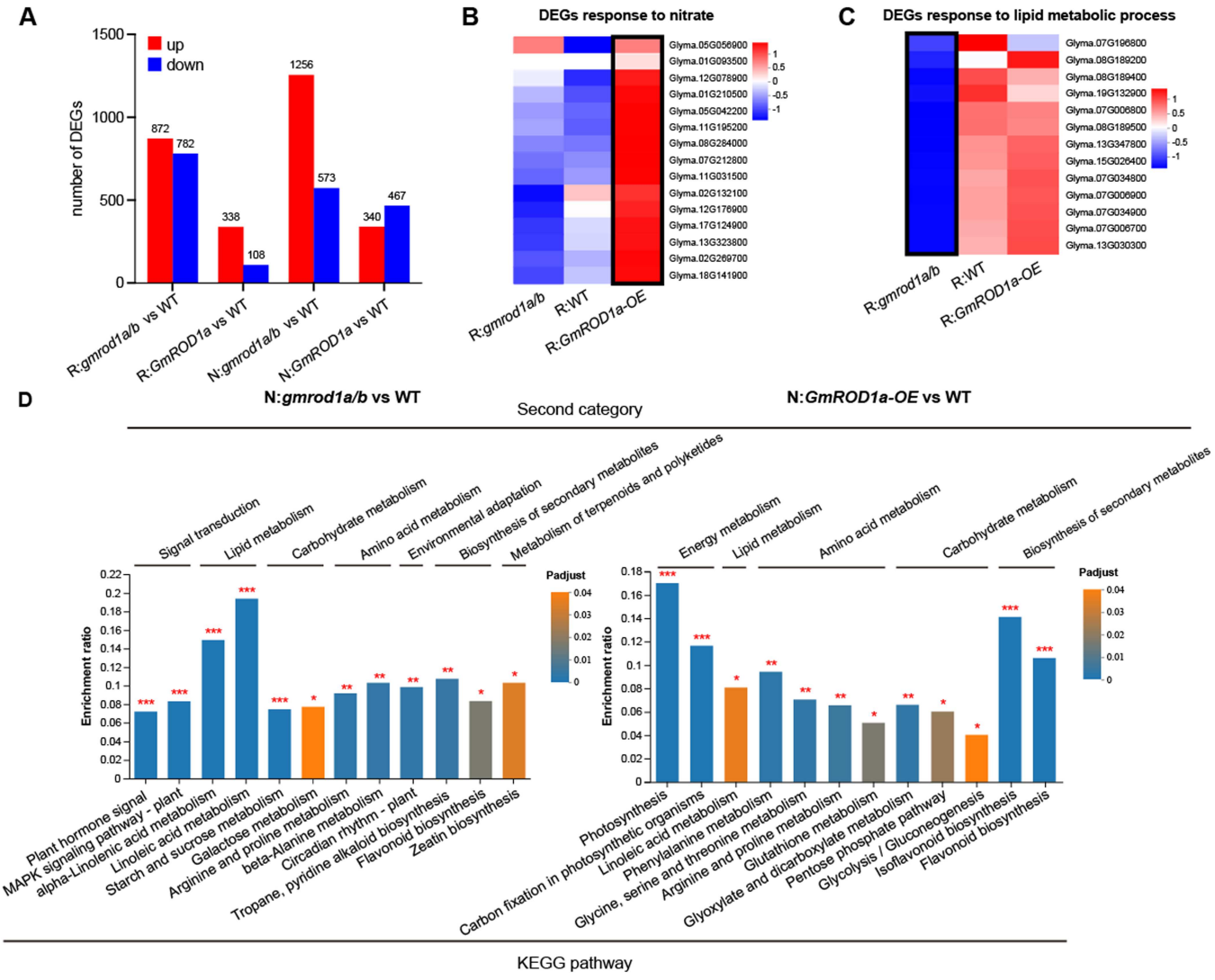

FIGURE 4 | Functional enrichment analysis of differentially expressed genes. (A) Numbers of differentially expressed genes (DEGs) in pairwise comparisons. (B) Heatmap of expression values of the DEGs in roots between *GmROD1a-OE* and WT that are enriched in the 'response to nitrate' term. (C) Heatmap of expression values of the DEGs in roots between *gmrod1a/b* and WT that are enriched in the 'lipid metabolic process' term. (D) Kyoto Encyclopaedia of Genes and Genomes (KEGG) enrichment analysis of genes that are differently expressed in nodules. The X-axis represents the pathway name, and the Y-axis represents the Rich factor (ratio of sample number of genes enriched in this pathway to background number of annotated genes), and the colour of the columns corresponds to different Padjust ranges. [Color figure can be viewed at wileyonlinelibrary.com]

processes (Supporting Information S1: Figure 7C,D). Consistently, Kyoto Encyclopaedia of Genes and Genomes (KEGG) enrichment analyses showed that DEGs from all four pairwise comparisons displayed significant enrichment for 'linoleic acid metabolism' (Figure 4D and Supporting Information S1: Figure 7E). The shared enrichment of lipid metabolic pathways across all four comparisons highlights a conserved lipid metabolic output regulated by GmROD1. Most enriched KEGG pathways were associated with lipid, amino acid and carbohydrate metabolism. Moreover, the DEGs between WT and *GmROD1a-OE* in roots and nodules were enriched for energy metabolism, which is tightly linked to nodulation (Figure 4D). Since lipid remodelling is tightly linked to membrane biogenesis and symbiotic interface formation, these results indicate that GmROD1s may coordinate nodulation by regulating lipid metabolism.

3.5 | GmWRI1 and GmWRI3 Act Upstream to Promote GmROD1s Expression

WRINKLED1 (WRI1), key regulators of lipid biosynthesis, functions as transcriptional activators by binding to AW-box motifs in the promoters of genes involved in fatty acid (FA) and triacylglycerol (TAG) production, such as PDCT (Chen et al. 2020). In the soybean genome, 15 AP2 domain-containing WRI1-like proteins were identified (Supporting Information S1: Figure 4), several of which are expressed in nodules (Supporting Information S1: Figure 5). Using both cDNA samples from rhizobium-inoculated roots and nodules, we were able to cloned two highly expressed transcripts, *GmWRI1*(*Glyma.15g221600*) and *GmWRI3* (*Glyma.08g220800*).

Yeast one-hybrid assays showed that both GmWRI1 and GmWRI3 interact with the promoters of *GmROD1a* and *GmROD1b* (Figure 5A). To validate these interactions in plants, we performed chromatin immunoprecipitation (ChIP) assays using *35S:GmWRI1/3-3FLAG* transgenic soybean hairy roots, as verified by Western blot (Figure 5B). ChIP-qPCR confirmed the binding of GmWRI1/3 to the *GmROD1* promoters, with enriched levels observed specifically in promoter fragments containing AW-box or GT1-box elements (Figure 5C–E). To examine whether GmWRI1/3 activate *GmROD1* transcription, we conducted transient dual-luciferase assays in tobacco leaves. Co-expression of GmWRI1 or GmWRI3 markedly increased the activities of the *GmROD1a* and *GmROD1b* promoters compared with the empty vector control, as indicated by elevated LUC reporter signals (Figure 5F–H). Together, these results indicated that GmWRI1 and GmWRI3 positively regulate the expression of *GmROD1* genes by directly binding to their promoters.

3.6 | GmWRI1 and GmWRI13 Regulate FA Accumulation and Nodulation in Soybean

To investigate the potential roles of GmWRI1 and GmWRI13 in soybean nodulation, we first examined their expression patterns in roots during rhizobial infection. Both genes displayed a marked induction at 48 h after inoculation (Figure 6A), suggesting that they may participate in early symbiotic signalling. To investigate their functional relevance, we generated transgenic soybean hairy roots overexpressing *GmWRI1* or *GmWRI13* under the CaMV *35S* promoter, and verified their elevated transcript levels by qRT-PCR (Supporting Information S1: Figure 6 Phenotypically, both OE lines exhibited enhanced nodulation capacity, including increased nodule numbers, higher ureide accumulation, and elevated total nitrogen content compared with empty vector (EV) controls (Figure 6D–H). Moreover, the expression of the early nodulation genes, including *GmNIN*, *GmNSP1*, *GmNSP2* and *GmNFR1*, was increased in the overexpression lines (Figure 6D,E), indicating that GmWRI1/3 promote early symbiotic signalling pathways. In addition, OE-GmWRI1 and OE-GmWRI3 roots accumulated significantly higher levels of total fatty acids (Figure 6I–L), aligning with the established role of WRI transcription factors in lipid biosynthesis. Taken together, these results demonstrated that GmWRI1 and GmWRI3 act as positive regulators of *GmROD1* genes and coordinately promote fatty acid accumulation and nodulation in soybean.

3.7 | GmROD1s Affect Plant Growth and Contribute to Soybean Yield

Under −N conditions with rhizobial inoculation, *GmROD1a*-overexpression plants exhibited markedly higher nitrogen content than WT, whereas mutants displayed reduced nitrogen content, accompanied by growth defects relative to WT (Figure 2). By contrast, under the +N condition, nitrogen content and shoot growth did not differ significantly among overexpression lines, mutants, and WT plants (Figure 2). underscore that the growth-promoting effect of GmROD1s is specifically dependent on symbiotic nitrogen fixation.

Seeking further insight into the contribution of GmROD1s to nodulation-driven growth, we performed hypocotyl grafting experiments in a greenhouse under nitrogen-deficient conditions with rhizobial inoculation. When WT shoots were grafted onto OE-GmROD1a rootstocks (WT onto OE-GmROD1a), nodulation was strongly promoted, accompanied by increases in plant height, ureide levels, and total nitrogen content (Figure 7A–E). In contrast, WT shoots grafted onto *gmrod1a/b* mutant roots (WT onto *gmrod1a/b*) showed compromised nodulation and reduced growth. Conversely, when roots of the WT plants served as rootstocks (WT onto WT; *OE-GmROD1a* onto WT; *gmrod1a/b* onto WT), both grafts formed similar numbers of nodules and displayed comparable nitrogen-fixing capacity (Figure 7). These grafting results demonstrate that root-expressed *GmROD1*s are important for enhancing nodulation and promoting shoot growth, consistent with phenotypes observed in stable transgenic soybean lines.

Subsequently, we employed a strategy involving chimeric soybean plants carrying *OE-GmROD1a* or *OE-GmROD1b* overexpressing transgenic hairy roots, as verified by qRT-PCR (Supporting Information S1: Figure 10). When grown under nitrogen-deficient conditions with rhizobia, these chimeric roots produced significantly more nodules than EV controls (Supporting Information S1: Figure 10E,F). Enhanced nodulation was accompanied by increased ureide accumulation and higher total nitrogen content in both OE-GmROD1a and OE-GmROD1b roots (Supporting Information S1: Figure 10G–I). Furthermore, the fatty acid profiles of these overexpression lines exhibited significant changes, including increased 18:2

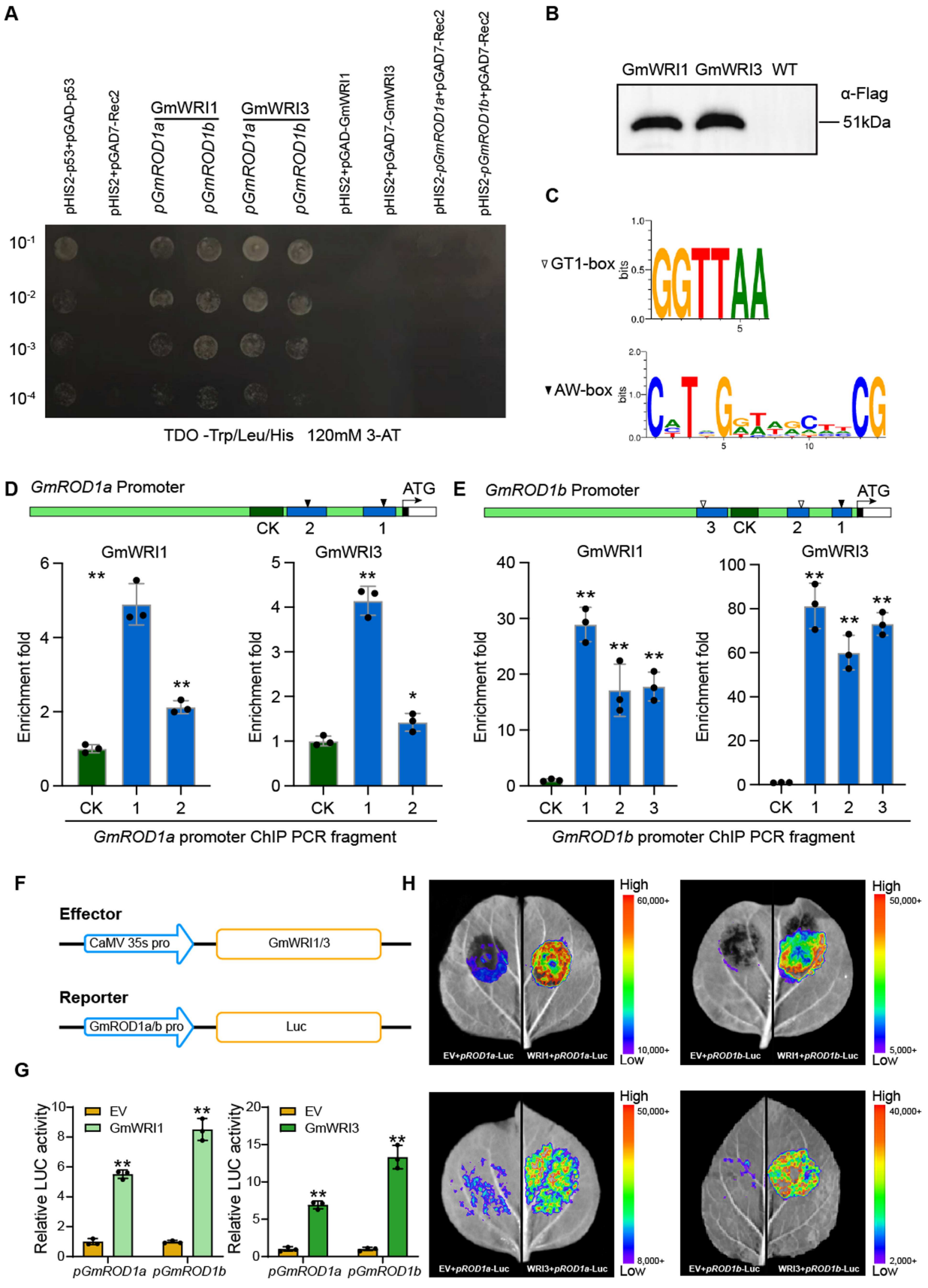

FIGURE 5 | Legend on next page.

levels and slight decreases in 16:0, 18:0, and 18:1. The chimeric soybean plants with *OE-GmROD1a* and *OE-GmROD1b* hairy roots exhibited a slight increase in plant height compared with EV controls (Supporting Information S1: Figure 10J,K).

Moreover, across multiple generations in greenhouse conditions and field trials conducted in Hainan and Zhejiang, *GmROD1* overexpression lines consistently produced higher yield per plant, further supporting the agronomic relevance of the GmROD1-regulated symbiotic pathway (Supporting Information S1: Figure 9 and Supporting Information S2: Table 2).

4 | Discussion

In soybean roots and nodules, the PUFAs are the most abundant FAs. As functional components of lipids and membranes, PUFAs are required for many biological processes, including rhizobia-legume symbiosis and nitrogen fixation. We found that the expression of *GmROD1s* in roots was highly induced by the rhizobial inoculation and remains high throughout in nodule development. Most importantly, our study identified GmROD1s as key enzymes in the desaturation of MUFAs to form PUFAs during TAG assembly in soybean and demonstrated the importance of *GmROD1a/b* for proper nodulation and nodule development. Furthermore, *GmROD1s* function downstream of GmWRI1 and GmWRI3, which mediated transcriptional regulation of FA synthesis and nodulation in roots and nodules. Notably, unlike GmWRI1, GmWRI3 has not previously been reported to function in nodulation, making its identification as another key regulator of soybean symbiosis a novel finding of this study. Taken together, our findings not only identify GmROD1s as FA desaturases in soybean but also shed light on *GmROD1*'s previously unknown contribution to nodulation and nodule development. Our study offered additional evidence supporting the role of lipid metabolism in regulating symbiosis in soybean.

ROD1 is closely linked to domestication and variety selection in both rice and soybean (Fang et al. 2017; Zhou et al. 2021). The mutation of *ROD1* in *Arabidopsis*, rapeseed and soybean seeds resulted in significant decreases in PUFA content in seeds (Lu et al. 2009; Bai et al. 2020; Li et al. 2023; Ulch et al. 2025), which is consistent with our results. The *GmROD1a*-overexpression lines displayed marked elevations in PUFA content in seeds, roots and nodules, especially for the C18:2, along with a considerable decrease in MUFA content. In the *GmROD1a*-overexpression lines, the lipid profiles of both rhizobia-inoculated roots and nodules showed steep increases in C18:2 and C18:3 which were carried by DAG and TAG, along with a concomitant decrease in C18:1 (Figure 3). KEGG enrichment analysis also showed that DEGs from the four pairwise comparisons in both roots and nodules were highly enriched for the 'linoleic acid metabolism' pathway (Figure 4D and Supporting Information S1: Figure 7E). Overall, these results suggested higher PUFAs flux into TAG in the *GmROD1a*-overexpression seeds and rhizobia-infected roots and nodules, where the *GmROD1s* are highly expressed (Figures 1 and 2).

Research in legumes implies that the process of rhizobial infection and nodulation requires the induction of membrane biogenesis in both the rhizobia and the host (López-Lara et al. 2003; Gaude et al. 2004; Strodtman et al. 2017). Previous study has shown that FAs (especially the PUFAs), phospholipids, and membrane lipid (monogalactosyldiacylglycerol, MGDG) biosynthesis in host root cells and their transport were required for nodulation and nodule structure (Gaude et al. 2004; Pii et al. 2009; Gillman et al. 2014; Krishnan et al. 2016; Lakhssassi et al. 2017, 2020; Chen et al. 2020; Zhang et al. 2020; Liu et al. 2023). During rhizobial infection, infection threads are formed and are fully enclosed by the host plasma membrane, thereby maintaining bacteria in an apoplastic compartment. Subsequent host cell enlargement and symbiosome proliferation require substantial membrane expansion (Lu et al. 2024). Membrane lipid remodelling is expected to influence membrane dynamics required for infection thread progression and symbiosome formation. Given that fatty acid unsaturation influences membrane fluidity, we hypothesise that increased PUFA levels may facilitate the membrane dynamics required for infection thread progression, symbiotic cells establishment and symbiosome proliferation. To further test our hypothesis, we examined symbiotic cell formation and nitrogen fixation capacity in different genetic backgrounds. Nodules at 21 dpi were stained with toluidine blue to visualise symbiotic phenotypes. Histological analysis revealed a significant reduction in symbiotic cell number in the *gmrod1a/b* mutants, whereas *GmROD1a* overexpression lines showed increased symbiotic cell abundance and enlarged cell size (Supporting Information S1: Figure 11). Consistent with these cellular phenotypes, we further examined nitrogenase accumulation and activity in nodules and found that both were significantly influenced by *GmROD1* expression levels (Supporting Information S1: Figure 12).

Given the established role of *ROD1* in fatty acid desaturation, it is plausible that ROD1-mediated PUFA remodelling influences

FIGURE 5 | The GmWRI1/3 transcription factors enhance the expression of GmROD1 genes by binding to their promoters. (A) The interaction between GmWRI1/3 and *GmROD1* promoters was tested in yeast one-hybrid assays. (B) Verification of GmWRI1 and GmWRI3 in transgenic hairy roots by Western blot. (C) Alignment of predicted GmWRI-binding promoter sequences identified using the web-based multiple expectation maximisation for motif elicitation (MEME) analysis program (http://meme-suite.org). The MEME search was performed using 1-kb upstream promoter sequences of genes previously reported to be bound by WRI transcription factors. The AW-box is represented by a filled triangle and the GT1-box is represented by an empty triangle. (D, E) Distribution of the binding elements in the promoter region of *GmROD1a* (D) and *GmROD1b* (E), with ChIP-qPCR analysis of the promoter of *GmROD1a* in *GmWRI1*-OE and *GmWRI3*-OE transgenic hairy roots. $n = 3$. 1,2,3,CK indicates different promoter fragments, the promoter fragments that did not contain any GT1-box or AW-box were used as CK. Experiments were conducted with three biological and two technical replicates. Data were expressed as means ± SD and presented normalised to CK. (F) Schematic diagrams of the effector and reporter constructs used for the tobacco transient expression assay. EV: empty vector. Data were presented normalised to EV. (G) Quantitative analysis of the luminescence intensity. $n = 3$. (H) Luciferase activity in tobacco leaves co-transfected with the constructs shown in (F). $n = 3$. Data are the means ± SD; significant differences ($^*p < 0.05$, $^{**}p < 0.01$) based on Student's *t*-test compared with CK or EV are indicated by asterisks. [Color figure can be viewed at wileyonlinelibrary.com]

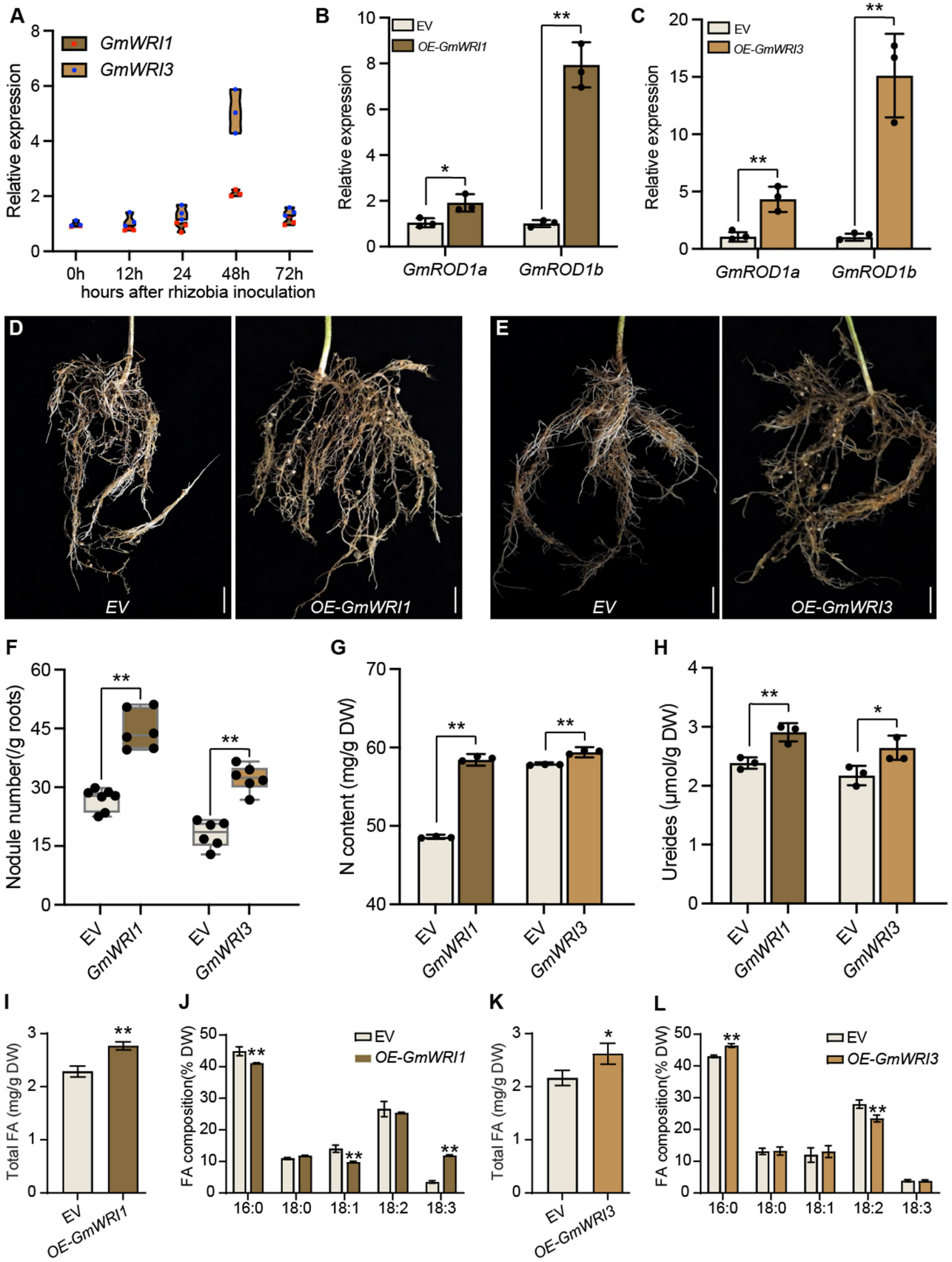

FIGURE 6 | Legend on next page.

membrane properties. Although due to technical limitations, we were unable to directly determine whether ROD1 alters membrane fluidity or structure, we examined changes in membrane lipid-related features. MGDGs, which are synthesised by MGDG synthase, encoded by *MGD1* and *MGD2*, are the primary components of the symbiosomal membranes in the inner nodules, where bacteroid differentiation and nitrogen fixation occur (Gaude et al. 2004; Kobayashi et al. 2009). Consistent with this, MGDG contents and the expression level of *GmMGD* genes were significantly up-regulated in *GmROD1a*-overexpression nodules (Supporting Information S1: Figure 8), indicating that ROD1-mediated lipid remodelling impacts the symbiotic interaction between rhizobia and host roots. Legumes interact with rhizobia that convert atmospheric nitrogen into ammonia for plant use (Udvardi and Poole 2013). Overexpressing *GmROD1*s caused markedly higher nitrogen content compared to WT plants in the presence of rhizobia, while mutants displayed a decrease in nitrogen content (Figure 2F). The most significantly enriched GO term between WT and *GmROD1a-OE* was 'response to nitrate' and DEGs related to 'response to nitrate' and 'nitrate transmembrane transport' were all up-regulated in the roots (Figure 4B and Supporting Information S1: Figure 7A–D). Moreover, the GO term 'regulation of nitrogen compound metabolic process' was significantly enriched in both infected roots and nodules between *gmrod1a/b* and WT (Supporting Information S1: Figure 7). Taken together, these results revealed that the GmROD1s affect nodulation in soybean.

Many metabolic genes are significantly regulated in response to rhizobial inoculation, including those related to FAs, amino acids, and carbohydrates (Brechenmacher et al. 2010; Libault et al. 2010; Udvardi and Poole 2013). Our transcriptomic analysis further supports this. The significantly enriched GO terms and KEGG pathway indicated GmROD1s' important role in FA synthesis and lipid metabolism (Figure 6 and Supporting Information S1: Figure 7). The GO terms were also enriched for several amino acid/carbohydrate-related metabolism in both roots and nodules between *gmrod1a/b* and WT (Figure 6B,F). Upon rhizobial infection, sucrose synthase and transporter genes were markedly induced, indicating that nodulation requires photosynthetically derived carbohydrates (Baier et al. 2007; Brechenmacher et al. 2008, 2010; Liu et al. 2023). These genes are activated to meet the metabolic and energy needs for early nodulation. In our data, several energy-related GO terms were enriched, including 'ADP binding', 'photosystem' and 'photosynthetic membrane' (Figure 4) and DEGs of the comparisons 'R:*GmROD1a-OE* vs. WT' and 'N:*GmROD1a-OE* vs. WT' were both enriched for 'energy metabolism' (Supporting Information S1: Figure 7). Moreover, the defence response-related terms and cell wall/membrane-related terms were markedly enriched in all groups (Figure 6), consistent with their established roles in nodulation (Brechenmacher et al. 2008; Libault et al. 2010). These results collectively show that manipulating *GmROD1*s expression in soybean has significant effects on multiple metabolic processes and gene expression networks that are important for nodulation, demonstrating that GmROD1s contribute to proper nodulation in soybean.

As key regulators of glycolysis and FA biosynthesis, the soybean *GmWRI1s* were induced by rhizobial infections and play key roles in nodulation and nodule development (Chen et al. 2020; Zheng et al. 2022). WRI proteins regulate glycolysis, FA synthesis, and TAG production by binding AW-box and GT1-box motifs (Tranbarger et al. 2011; Wu et al. 2014). We identified AW- and GT1-box motifs in the promoters of *GmROD1a/b* (Figure 5C–E). We found that both *GmWRI1* and *GmWRI3* are expressed in infected roots and nodules and can promote *GmROD1*s transcription by directly binding to their promoters (Figure 5). Importantly, GmWRI3 has not previously been implicated in nodulation, making its identification as a regulator of soybean symbiosis another key discovery of this study. We further confirmed that GmWRI1 and GmWRI3 played important roles in FA accumulation and nodulation through transgenic soybean hairy roots assays (Figure 6 and Supporting Information S1: Figure 6).

Enhanced nodulation can contribute to improved productivity in legume crops. Legume nodules provide a specialised niche for nitrogen-fixing bacteria, where atmospheric N_2 is reduced into biologically usable forms through symbiotic nitrogen fixation. Symbiotic nitrogen fixation represents a major source of nitrogen for soybean production systems. Analyses of nitrogen budgets indicate that biological nitrogen fixation can supply a substantial proportion of crop nitrogen demand in soybean-based agroecosystems. On an average, 50%–60% of soybean N demand was met by symbiotic nitrogen fixation (Salvagiotti et al. 2008). Consistent with this view, field studies have shown that enhancing nodulation efficiency through rhizobial inoculation can significantly increase nitrogen fixation and grain yield (Serafin-Andrzejewska et al. 2024). Through symbiotic relationships, *Bradyrhizobium* helps plants to mobilise nutrients, produce phytohormones, and enhance stress tolerance by antioxidative mechanisms, ultimately contributing to improved agricultural productivity (Chiurazzi et al. 2025; Sharma et al. 2026). A number of studies have reported that genetic manipulation of nodulation-related genes can enhance soybean productivity by improving symbiotic nitrogen fixation (Qin et al. 2012; Chen et al. 2019; Yang et al. 2022).

In our study, knockout of *GmROD1* minimally affected soybean growth under non-symbiotic conditions, but dramatically impaired

FIGURE 6 | Overexpressing GmWRI1 and GmWRI13 in soybean hairy roots promotes nodulation. (A) Expression pattern of *GmWRI1* and *GmWRI3* in roots during rhizobial inoculation. Data were expressed as means ± SD and presented normalised to 0 h. Experiments were conducted with three biological and two technical replicates. (B, C) qRT-PCR verification of *GmROD1s* transcript levels in *OE-GmWRI1* (B) and *OE-GmWRI1* (C) transgenic hairy roots. Data were expressed as means ± SD and presented normalised to EV. Experiments were conducted with three biological and two technical replicates. (D, E) Nodulation of the EV, *OE-GmWRI1* (D) and *OE-GmWRI13* (E) transgenic hairy roots _ days after infection with rhizobia. Scale bar, 2 cm. (F–H) Quantitative analysis of nodule number (F), nitrogen content (G) and ureide content (H) of *OE-GmWRI1* and *OE-GmWRI3* transgenic chimeric soybean plants. $n = 6$. (I, J) Total FA content (I) and FA composition (J) of *OE-GmWRI1* transgenic hairy roots. $n = 3$. (K, L) Total FA content (K) and FA composition (L) of *OE-GmWRI3* transgenic hairy roots. $n = 3$. DW: dry weight; EV: empty vector. Data are the means ± SD; significant differences ($^*p < 0.05$, $^{**}p < 0.01$) based on Student's *t*-test compared with EV are indicated by asterisks. [Color figure can be viewed at wileyonlinelibrary.com]

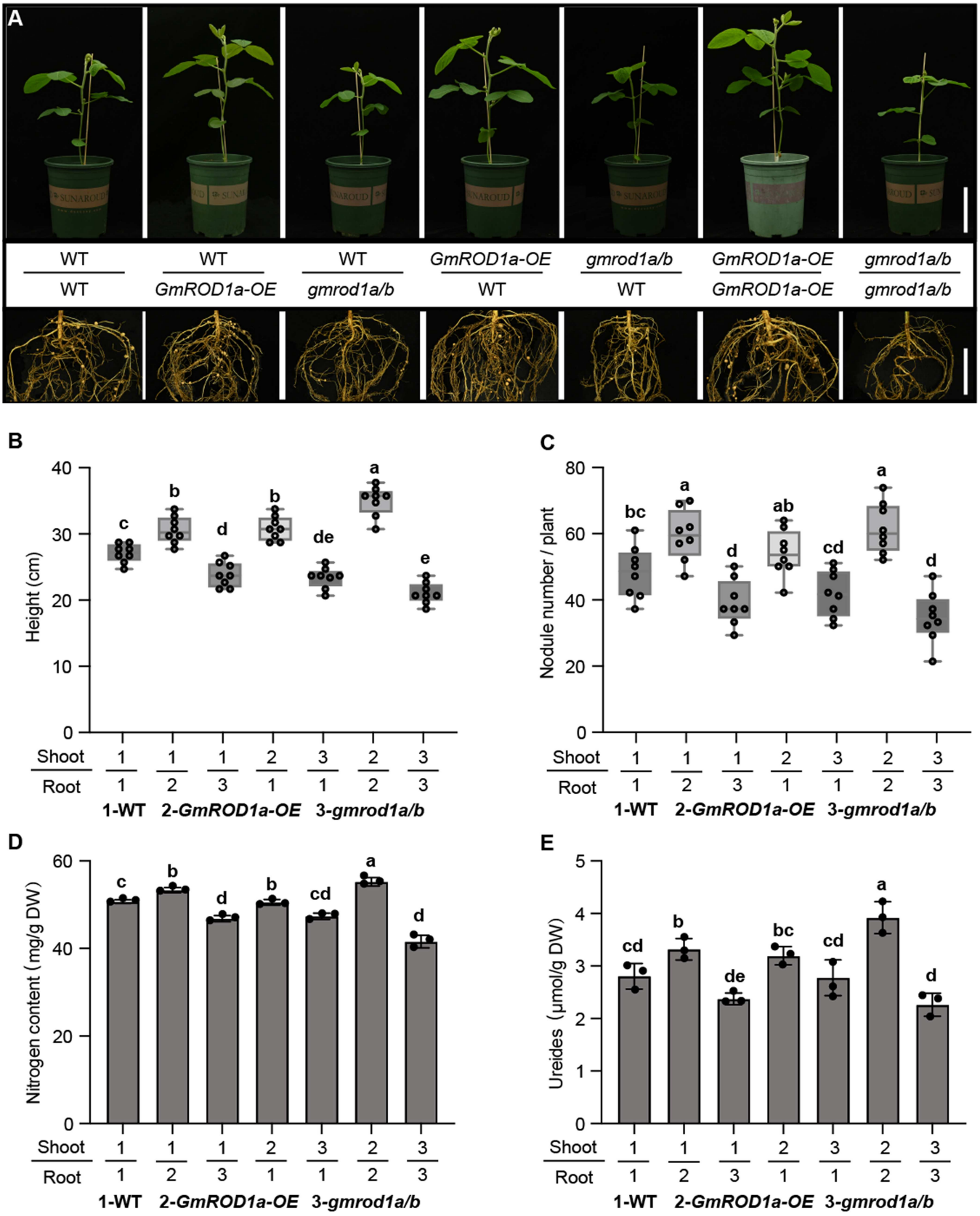

FIGURE 7 | Effects of GmROD1 overexpression on nodulation and plant growth in shoot–root grafts. (A) Growth performance of shoot–root grafts. Scale bar of shoots, 10 cm; scale bar of roots, 5 cm. (B, C) Height (B) and nodule number (C) of shoot–root grafts. $n = 8$. (D, E) Nitrogen content (D) and ureide content (E) of shoot–root grafts. $n = 3$. Seedlings that survived/ hypocotyl grafting were inoculated with *B. japonicum* USDA100 rhizobia and incubated in vermiculite for 28 days before sampling for measurement. 1: wild type soybean (WT); 2: *GmROD1a*-overexpression transgenic soybean; 3: *gmrod1a/b* mutant. Data are means ± SD; significant differences were determined by one-way ANOVA analysis with Duncan's multiple comparison tests, and different letters indicate a significant difference ($p < 0.05$). [Color figure can be viewed at wileyonlinelibrary.com]

nodulation, slowed nodule development and diminished SNF activity under nitrogen-deficient and rhizobia-inoculated conditions, which eventually led to negative effects on growth (Figure 2). Conversely, *GmROD1* overexpression improved nodule development, resulting in a significant increase in soybean plant growth in the field (Figure 3, Supporting Information S1: Figure 9 and Supporting Information S2: Table 2). And grafting experiments using stable transgenic lines further confirmed that proper, improved nodulation resulting from overexpressing *GmROD1* had positive effects on plant growth (Supporting Information S1: Figure 10). ROD1-mediated changes in PUFA metabolism were associated with increased nodulation and nitrogenase accumulation, suggesting that improved symbiotic nitrogen fixation likely contributes to the enhanced growth and yield observed in the field trials. However, lipid metabolism also plays broader roles in plant development and carbon allocation. Therefore, we cannot exclude the possibility that altered lipid metabolism may additionally influence plant growth through mechanisms independent of symbiosis.

Since we didn't generate stable *GmROD1b*-overexpressing transgenic plants, we employed a strategy involving chimeric soybean plants with *GmROD1a*- and *GmROD1b*-overexpressing hairy roots. Our results support partially redundant functions of *GmROD1a* and *GmROD1b* in root fatty acid desaturation (Supporting Information S1: Figure 10J,K) and both influence nodulation-related phenotypes and plant growth to some extent (Supporting Information S1: Figure 10A–I). Notably, several observations point to some differences in the regulation of the two paralogs. First, although the two genes exhibit broadly similar expression patterns in both seeds and nodules, *GmROD1a* is expressed at substantially higher levels than *GmROD1b* (approximately threefold; Figure 1A), suggesting that it may contribute more prominently under the tested conditions. Second, following rhizobial inoculation, *GmROD1a* displays an earlier induction peak (5 dpi) than *GmROD1b* (7 dpi) (Figure 1B). In addition, the *GmROD1b* promoter contains more predicted WRI-binding elements and exhibits stronger transcriptional responsiveness to WRIs (Figures 5, and 6B,C).

In conclusion, this study expands our understanding of GmROD1 functions, revealing that they are required not only for fatty acid desaturation but also for proper nodulation and nodule development. Our work provides a new perspective on the molecular mechanism through which GmWRIs dynamically and precisely regulate lipid biosynthesis and nodulation in soybean. Furthermore, this work provides evidence that links fatty acid desaturation with nodulation, providing new insights into the metabolic control of the soybean–rhizobia symbiosis.

Acknowledgements

This work was supported by Kunpeng Program of Zhejiang provincial government, the National Natural Science Foundation of China (32572127), China Postdoctoral Science Foundation (2025M784053), Zhejiang Province Postdoctoral Research Project Selective Funding Program (ZJ2025067).

Data Availability Statement

The data that support the findings of this study are openly available in NCBI Sequence Read Archive (SRA) at https://www.ncbi.nlm.nih.gov/sra, reference number PRJNA1435896.

References

Abdullah, H. M., N. Pang, B. Chilcoat, Y. Shachar-Hill, D. J. Schnell, and O. P. Dhankher. 2024. "Overexpression of the *Phosphatidylcholine:Diacylglycerolcholinephosphotransferase (PDCT)* Gene Increases Carbon Flux Toward Triacylglycerol (TAG) Synthesis in *Camelina sativa* Seeds." *Plant Physiology and Biochemistry* 208: 108470.

Andrews, M., and M. E. Andrews. 2017. "Specificity in Legume-Rhizobia Symbioses." *International Journal of Molecular Sciences* 18, no. 4: 705.

Bai, S., J. G. Wallis, P. Denolf, et al. 2020. "The Biochemistry of Headgroup Exchange During Triacylglycerol Synthesis in Canola." *Plant Journal* 103, no. 1: 83–94.

Baier, M. C., A. Barsch, H. Küster, and N. Hohnjec. 2007. "Antisense Repression of the *Medicago truncatula* Nodule-Enhanced Sucrose Synthase Leads to a Handicapped Nitrogen Fixation Mirrored by Specific Alterations in the Symbiotic Transcriptome and Metabolome." *Plant Physiology* 145, no. 4: 1600–1618.

Bates, P. D., A. Fatihi, A. R. Snapp, A. S. Carlsson, J. Browse, and C. Lu. 2012. "Acyl Editing and Headgroup Exchange Are the Major Mechanisms That Direct Polyunsaturated Fatty Acid Flux Into Triacylglycerols." *Plant Physiology* 160, no. 3: 1530–1539.

Bourassa, D. V., E. L. Kannenberg, D. J. Sherrier, R. J. Buhr, and R. W. Carlson. 2017. "The Lipopolysaccharide Lipid a Long-Chain Fatty Acid Is Important for *Rhizobium leguminosarum* Growth and Stress Adaptation in Free-Living and Nodule Environments." *Molecular Plant–Microbe Interactions* 30, no. 2: 161–175.

Brands, M., V. Wewer, A. Keymer, C. Gutjahr, and P. Dörmann. 2018. "The *Lotus japonicus* Acyl–Acyl Carrier Protein Thioesterase FatM Is Required for Mycorrhiza Formation and Lipid Accumulation of *Rhizophagus irregularis*." *Plant Journal* 95, no. 2: 219–232.

Bravo, A., M. Brands, V. Wewer, P. Dörmann, and M. J. Harrison. 2017. "Arbuscular Mycorrhiza-Specific Enzymes FatM and RAM2 Fine-Tune Lipid Biosynthesis to Promote Development of Arbuscular Mycorrhiza." *New Phytologist* 214, no. 4: 1631–1645.

Bravo, A., T. York, N. Pumplin, L. A. Mueller, and M. J. Harrison. 2016. "Genes Conserved for Arbuscular Mycorrhizal Symbiosis Identified Through Phylogenomics." *Nature Plants* 2: 15208.

Brechenmacher, L., M. Y. Kim, M. Benitez, et al. 2008. "Transcription Profiling of Soybean Nodulation by *Bradyrhizobium japonicum*." *Molecular Plant–Microbe Interactions* 21, no. 5: 631–645.

Brechenmacher, L., Z. Lei, M. Libault, et al. 2010. "Soybean Metabolites Regulated in Root Hairs in Response to the Symbiotic Bacterium *Bradyrhizobium japonicum*." *Plant Physiology* 153, no. 4: 1808–1822.

Chen, B., G. Zhang, P. Li, et al. 2020. "Multiple *GmWRI1s* Are Redundantly Involved in Seed Filling and Nodulation by Regulating Plastidic Glycolysis, Lipid Biosynthesis and Hormone Signalling in Soybean (*Glycine max*)." *Plant Biotechnology Journal* 18, no. 1: 155–171.

Chen, L., L. Qin, L. Zhou, et al. 2019. "A Nodule-Localized Phosphate Transporter GmPT7 Plays an Important Role in Enhancing Symbiotic N(2) Fixation and Yield in Soybean." *New Phytologist* 221, no. 4: 2013–2025.

Chiurazzi, M., G. Frugis, and L. Navazio. 2025. "Symbiotic Nitrogen Fixation: A Launchpad for Investigating Old and New Challenges." *Journal of Experimental Botany* 76, no. 6: 1473–1477.

Delves, A. C., A. Mathews, D. A. Day, A. S. Carter, B. J. Carroll, and P. M. Gresshoff. 1986. "Regulation of the Soybean-Rhizobium Nodule Symbiosis by Shoot and Root Factors." *Plant Physiology* 82, no. 2: 588–590.

Fang, C., Y. Ma, S. Wu, et al. 2017. "Genome-Wide Association Studies Dissect the Genetic Networks Underlying Agronomical Traits in Soybean." *Genome Biology* 18, no. 1: 161.

Gaude, N., H. Tippmann, E. Flemetakis, P. Katinakis, M. Udvardi, and P. Dörmann. 2004. "The Galactolipid Digalactosyldiacylglycerol Accumulates in the Peribacteroid Membrane of Nitrogen-Fixing Nodules of Soybean and Lotus." *Journal of Biological Chemistry* 279, no. 33: 34624–34630.

Gillman, J. D., M. G. Stacey, Y. Cui, H. R. Berg, and G. Stacey. 2014. "Deletions of the *SACPD-C* Locus Elevate Seed Stearic Acid Levels but Also Result in Fatty Acid and Morphological Alterations in Nitrogen Fixing Nodules." *BMC Plant Biology* 14: 143.

Guo, W., J. Zhao, X. Li, L. Qin, X. Yan, and H. Liao. 2011. "A Soybean β-Expansin Gene GmEXPB2 Intrinsically Involved in Root System Architecture Responses to Abiotic Stresses." *Plant Journal* 66, no. 3: 541–552.

Jiang, Y., W. Wang, Q. Xie, et al. 2017. "Plants Transfer Lipids to Sustain Colonization by Mutualistic Mycorrhizal and Parasitic Fungi." *Science* 356, no. 6343: 1172–1175.

Kereszt, A., D. Li, A. Indrasumunar, et al. 2007. "Agrobacterium Rhizogenes-Mediated Transformation of Soybean to Study Root Biology." *Nature Protocols* 2, no. 4: 948–952.

Kobayashi, K., K. Awai, M. Nakamura, A. Nagatani, T. Masuda, and H. Ohta. 2009. "Type-B Monogalactosyldiacylglycerol Synthases Are Involved in Phosphate Starvation-Induced Lipid Remodeling, and Are Crucial for Low-Phosphate Adaptation." *Plant Journal* 57, no. 2: 322–331.

Krishnan, H. B., A. A. Alaswad, N. W. Oehrle, and J. D. Gillman. 2016. "Deletion of the *SACPD-C* Locus Alters the Symbiotic Relationship Between *Bradyrhizobium japonicum* USDA110 and Soybean, Resulting in Elicitation of Plant Defense Response and Nodulation Defects." *Molecular Plant-Microbe Interactions* 29, no. 11: 862–877.

Lakhssassi, N., V. Colantonio, N. D. Flowers, et al. 2017. "Stearoyl-Acyl Carrier Protein Desaturase Mutations Uncover an Impact of Stearic Acid in Leaf and Nodule Structure." *Plant Physiology* 174, no. 3: 1531–1543.

Lakhssassi, N., Z. Zhou, S. Liu, et al. 2020. "Soybean TILLING-by-Sequencing+ Reveals the Role of Novel *GmSACPD* Members in Unsaturated Fatty Acid Biosynthesis While Maintaining Healthy Nodules." *Journal of Experimental Botany* 71, no. 22: 6969–6987.

Li, H., R. Zhou, P. Liu, et al. 2023. "Design of High-Monounsaturated Fatty Acid Soybean Seed Oil Using GmPDCTs Knockout via a CRISPR-Cas9 System." *Plant Biotechnology Journal* 21, no. 7: 1317–1319.

Liao, W., R. Guo, K. Qian, W. Shi, J. Whelan, and H. Shou. 2024. "The Acyl–Acyl Carrier Protein Thioesterases GmFATA1 and GmFATA2 Are Essential for Fatty Acid Accumulation and Growth in Soybean." *Plant Journal* 118, no. 3: 823–838.

Libault, M., A. Farmer, L. Brechenmacher, et al. 2010. "Complete Transcriptome of the Soybean Root Hair Cell, a Single-Cell Model, and Its Alteration in Response to *Bradyrhizobium japonicum* Infection." *Plant Physiology* 152, no. 2: 541–552.

Liu, Z., X. Kong, Y. Long, et al. 2023. "Integrated Single-Nucleus and Spatial Transcriptomics Captures Transitional States in Soybean Nodule Maturation." *Nature Plants* 9, no. 4: 515–524.

López-Lara, I. M., C. Sohlenkamp, and O. Geiger. 2003. "Membrane Lipids in Plant-Associated Bacteria: Their Biosyntheses and Possible Functions." *Molecular Plant–Microbe Interactions* 16, no. 7: 567–579.

Lu, C., Z. Xin, Z. Ren, M. Miquel, and J. Browse. 2009. "An Enzyme Regulating Triacylglycerol Composition Is Encoded by the ROD1 Gene of Arabidopsis." *Proceedings of the National Academy of Sciences of the United States of America* 106, no. 44: 18837–18842.

Lu, W., X. Wang, and W. Jia. 2024. "Characterization of Root Hair Curling and Nodule Development in Soybean-Rhizobia Symbiosis." *Sensors* 24, no. 17: 5726.

Pii, Y., A. Astegno, E. Peroni, M. Zaccardelli, T. Pandolfini, and M. Crimi. 2009. "The *Medicago truncatula* N5Gene Encoding a Root-Specific Lipid Transfer Protein Is Required for the Symbiotic Interaction With *Sinorhizobium meliloti*." *Molecular Plant–Microbe Interactions* 22, no. 12: 1577–1587.

Qin, L., J. Zhao, J. Tian, et al. 2012. "The High-Affinity Phosphate Transporter GmPT5 Regulates Phosphate Transport to Nodules and Nodulation in Soybean." *Plant Physiology* 159, no. 4: 1634–1643.

Rich, M. K., N. Vigneron, C. Libourel, et al. 2021. "Lipid Exchanges Drove the Evolution of Mutualism During Plant Terrestrialization." *Science* 372, no. 6544: 864–868.

Salvagiotti, F., K. G. Cassman, J. E. Specht, D. T. Walters, A. Weiss, and A. Dobermann. 2008. "Nitrogen Uptake, Fixation and Response to Fertilizer N in Soybeans: A Review." *Field Crops Research* 108, no. 1: 1–13.

Serafin-Andrzejewska, M., A. Jama-Rodzeńska, W. Helios, et al. 2024. "Influence of Nitrogen Fertilization, Seed Inoculation and the Synergistic Effect of These Treatments on Soybean Yields under Conditions in South-Western Poland." *Scientific Reports* 14, no. 1: 6672.

Sharma, R., D. Kumar, N. Kapoor, and P. Ohri. 2026. "Insights into the Biodiversity, Mechanisms and Plant Growth-Promoting Effects of *Bradyrhizobium* and Its Potential in Sustainable Agriculture: A Review." *Pedosphere* 36, no. 1: 147–164.

Strodtman, K. N., S. E. Stevenson, J. K. Waters, et al. 2017. "The Bacteroid Periplasm in Soybean Nodules Is an Interkingdom Symbiotic Space." *Molecular Plant–Microbe Interactions* 30, no. 12: 997–1008.

Tegeder, M. 2014. "Transporters Involved in Source to Sink Partitioning of Amino Acids and Ureides: Opportunities for Crop Improvement." *Journal of Experimental Botany* 65, no. 7: 1865–1878.

Tranbarger, T. J., S. Dussert, T. Joët, et al. 2011. "Regulatory Mechanisms Underlying Oil Palm Fruit Mesocarp Maturation, Ripening, and Functional Specialization in Lipid and Carotenoid Metabolism." *Plant Physiology* 156, no. 2: 564–584.

Udvardi, M., and P. S. Poole. 2013. "Transport and Metabolism in Legume-Rhizobia Symbioses." *Annual Review of Plant Biology* 64: 781–805.

Ulch, B. A., A. C. Clews, M. W. Jesionowska, M. S. Kimber, R. T. Mullen, and Y. Xu. 2025. "Characterization of Phosphatidylcholine:Diacylglycerol Cholinephosphotransferases From Soybean (*Glycine max*)." *Journal of Agricultural and Food Chemistry* 73, no. 13: 7645–7657.

Upchurch, R. G. 2008. "Fatty Acid Unsaturation, Mobilization, and Regulation in the Response of Plants to Stress." *Biotechnology Letters* 30, no. 6: 967–977.

Wang, J., K. Tóth, K. Tanaka, et al. 2014. "A Soybean Acyl Carrier Protein, GmACP, Is Important for Root Nodule Symbiosis." *Molecular Plant–Microbe Interactions* 27, no. 5: 415–423.

Wu, F., and Y. Hanzawa. 2018. "A Simple Method for Isolation of Soybean Protoplasts and Application to Transient Gene Expression Analyses." *Journal of Visualized Experiments: JoVE* no. 131: 57258.

Wu, X. L., Z. H. Liu, Z. H. Hu, and R. Z. Huang. 2014. "BnWRI1 Coordinates Fatty Acid Biosynthesis and Photosynthesis Pathways During Oil Accumulation in Rapeseed." *Journal of Integrative Plant Biology* 56, no. 6: 582–593.

Yang, Z., H. Du, X. Xing, et al. 2022. "A Small Heat Shock Protein, GmHSP17.9, From Nodule Confers Symbiotic Nitrogen Fixation and Seed Yield in Soybean." *Plant Biotechnology Journal* 20, no. 1: 103–115.

Zhang, G., M. Z. Ahmad, B. Chen, et al. 2020. "Lipidomic and Transcriptomic Profiling of Developing Nodules Reveals the Essential Roles of Active Glycolysis and Fatty Acid and Membrane Lipid Biosynthesis in Soybean Nodulation." *Plant Journal* 103, no. 4: 1351–1371.

Zheng, H., D. Zhao, and W. Shao, et al. 2022. "GmWRI1c Increases Palmitic Acid Content to Regulate Seed Oil Content and Nodulation in Soybean (*Glycine max*)." *International Journal of Molecular Sciences* 23, no. 22: 13793.

Zhou, H., D. Xia, P. Li, et al. 2021. "Genetic Architecture and Key Genes Controlling the Diversity of Oil Composition in Rice Grains." *Molecular Plant* 14, no. 3: 456–469.

Supporting Information

Additional supporting information can be found online in the Supporting Information section.

Figure S1: Phylogenetic analysis of ROD1 family members in soybean, together with other ROD1 members that have been reported in plants.
Figure S2: Expression patterns of GmROD1a and GmROD1b in soybean plants.
Figure S3: Identification of gmrod1a/b mutant and GmROD1a-over-expression lines.
Figure S4: Phylogenetic analysis of GmWRIs in soybean.
Figure S5: Expression pattern analysis of GmWRIs in soybean.
Figure S6: Overexpressing GmWRI1 and GmWRI3 in soybean hairy roots.
Figure S7: Functional enrichment analysis of DEGs.
Figure S8: Effects of GmROD1 overexpression on the abundance of MGDGs.
Figure S9: Effects of overexpressing and knocking out GmROD1s on plant growth in soybean.
Figure S10: Effects of overexpressing GmROD1a and GmROD1b in hairy roots.
Figure S11: Structure of infected cells.
Figure S12: Effects of GmROD1 on nitrogen fixation capacity.
Table S1: The accession numbers of genes and primer sequences for qRT-PCR primers used in this study.
Table S2: Statistics of agronomic traits.